Polymer Testing 103 (2021) 107347

Contents lists available at ScienceDirect

Polymer Testing

journal homepage: www.elsevier.com/locate/polytest

# Investigation of the damping properties of polylactic acid-based syntactic foam structures

Katalin Litauszki [a], Ákos Kmetty [a,b,*]

[a] Department of Polymer Engineering, Faculty of Mechanical Engineering, Budapest University of Technology and Economics, Műegyetem rkp. 3., H-1111, Budapest, Hungary

[b] MTA–BME Research Group for Composite Science and Technology, Műegyetem rkp. 3, H-1111, Budapest, Hungary

ARTICLE INFO

*Keywords:*
Damping
Syntactic foam
Polylactic acid
Extrusion
Physical blowing agent

ABSTRACT

Nowadays, environmental awareness is more and more important. Therefore, the importance of weight reduction and creating a circular economy has increased. In this study, we foamed bio-based polylactic acid (PLA) with thermally expandable microspheres to create homogenous, compostable polymer foams. The polylactic acid-based foamed sheet samples were produced with a flat sheet extruder at 190 °C. We investigated the temperature-dependent mechanical properties of the samples—they show maximum damping capacity in the glass transition region. We also examined the frequency-dependent properties of the foamed samples and successfully extended these properties with the time-temperature superposition principle, to broaden the potential field of application of the foams. The damping properties of homogeneous, closed-cell foam structures produced with thermally expandable microspheres increased in the range of 0.1–20 000 Hz as a function of foaming agent content. We also produced foamed sheets from PLA/PBAT (polybutylene succinate) blends. The storage modulus of unfoamed reference samples showed a decreasing tendency. The tanδ of foamed systems containing only PLA or PBAT increased. The tanδ of foamed blends decreased in 25%/75% and 50%/50%PBAT/PLA systems, except for the 75%/25%PBAT/PLA blend. Therefore, PBAT/PLA blends can only be used to improve the damping ability of foamed samples above 75 wt% PBAT.

## 1. Introduction

Biopolymers offer a promising alternative to conventional polymers in some applications (e.g. short life cycle products). However, their application areas are not well defined yet [1]. Polylactic acid and their foams are brittle and this is a problem to be solved. The importance of polymer foams is growing [2]. One of the main properties of foams is their energy absorbing and damping ability, therefore it is important to study and develop these properties in polylactic acid-based foams as well. Foaming with thermally expandable microspheres (EMS) is a very promising method among continuous foaming technologies. EMS can be used to create medium-density biopolymer foams with a homogeneous cell structure [3]. In general, an important feature of foam structures is their outstanding energy absorption capacity, and sound and vibration damping, therefore it is very important to study these properties [4,5]. Examples of vibrations that occur in practice are whole-body and hand-transmitted vibrations, which have a frequency range of 1–80 Hz for whole-body vibrations and 8–1250 Hz for hand-transmitted vibrations [6]. The frequency range of audible sound is 20 to 20 000 Hz [7]. The vibration frequencies of trucks range from 3 to 55 Hz [8]. The deployment of the airbags in the event of an accident means a frequency of approximately 10 000 Hz [9]. The damping and energy-absorbing properties of foam structures can be investigated with dynamic mechanical methods. Examples of dynamic mechanical tests are dynamic mechanical analysis (DMA) [10], and drop spear and falling weight tests. The great advantage of the dynamic mechanical analysis is that it can be used to obtain information on the viscoelastic properties of the material over a wide frequency range (0.01–100 Hz). A DMA test can be used to determine the storage modulus (E′), loss modulus (E′′) and damping factor (tanδ) of a material, which can be defined as the quotient of the loss factor and the storage modulus [11,12]. To date, in most research, DMA tests have been conducted at a constant frequency of 1 Hz as a function of temperature, thus showing the temperature-dependent properties of materials and foam structures [13–16]. The simplest and

* Corresponding author. Department of Polymer Engineering, Faculty of Mechanical Engineering, Budapest University of Technology and Economics, Műegyetem rkp. 3., H-1111, Budapest, Hungary.
*E-mail address:* kmetty@pt.bme.hu (Á. Kmetty).

https://doi.org/10.1016/j.polymertesting.2021.107347
Received 16 April 2021; Received in revised form 23 August 2021; Accepted 10 September 2021
Available online 11 September 2021

most common method to collect frequency data is to keep the temperature constant and perform frequency sweeps in the desired frequency range. Preferably, at the specified frequencies, for example at 1 Hz, 2.5 Hz, 5 Hz and 10 Hz. This provides a good overview of the test results when displayed on a logarithmic scale [9]. This frequency sweep test can be performed on a series of isotherms [9] then, using the principle of time–temperature superposition (TTS). The test results can then be extended to a wider range of frequencies for a given reference temperature ($T_{ref}$). The basic principle of the TTS method is that values measured at low frequencies are equivalent to the values measured at high temperatures ($T \geq T_{ref}$), and the values at high frequency are equivalent to the values measured at low temperatures ($T < T_{ref}$) [17]. The applied temperature-dependent frequency shift factor ($a_T$) can be determined below the glass transition temperature ($T_g$) with the Arrhenius equation and above the glass transition temperature with the empirical WLF equation [7]. In the case of polymeric foam structures, only a small number of publications investigate extended frequency-dependent properties. An example of this is the paper of Briatico-Vangosa et al. [7]. They investigated the sound absorption capacity of flexible polyurethane-based open-cell foam structures. Two polyurethane foams with different densities (31.2 kg/m$^3$ and 94.6 kg/m$^3$) were tested in their study. They used dynamic mechanical tests with a compression fixture and successfully applied TTS on the measured loss factor values. The availability of these results may help to broaden the scope of application of biopolymers. Our goal was to investigate the damping properties of homogeneous cellular biopolymer-based foam structures produced by extrusion with the use of thermally expandable microspheres. We took into account the effect of the D-lactide content of the polylactic acid. We produced PLA foams with low, medium and high D-lactide content with an EMS foaming agent. We classified the foam structures thus produced in terms of product geometry, density and cell morphology. Next, we characterized the temperature-dependent attenuation properties of PLA-based samples at 1 Hz, which is common in the literature. Then, damping properties were tested at room temperature as a function of frequency (frequency sweep). In the next step, we determined the required isothermals, where we also carried out the frequency sweeps. Using these measurement points, we generated the master curve and extended the test frequency range using the TTS method. Finally, we reduced the rigidity of polylactic acid-based syntactic foam structures by mixing polybutylene PBAT (a flexible compostable biopolymer) into the PLA.

## 2. Materials and methods

### 2.1. Materials

For the PLA based foams, we used Ingeo 4032D, 2003D and 4060D (NatureWorks, USA) PLA, with 1.4, 4.3 and 12.0 mol% D-lactide content, respectively [18]. The density of the PLAs is 1.24 g/cm$^3$ [19,20]. In the case of semi-crystalline PLA, $T_g$ is 65 °C (4032D) and 61 °C (2003D). In the case of amorphous PLA with 12% D-lactide content, $T_g$ is 58 °C and differential scanning calorimetry did not detect $T_m$ [21]. We used Tracel G 6800 MS thermally expandable microspheres (EMS) as a physical blowing agent from Tramaco GmbH (Germany). We examined the EMS foaming agent in detail in our previous publications [3,21]. The amounts of EMS were 0.5, 1, 2, 4 and 8 wt%.

We developed PLA/PBAT binary blends for polymer foam systems for increased damping capacity. PBAT is a biodegradable aliphatic-aromatic copolyester. We used Ecoflex® F Blend C1200 manufactured by BASF (Ludwigshafen, Germany). Its density is 1.26 ± 0.01 g/cm$^3$ [22]. The PLA component in this case was Ingeo 2003D. Prior to foam extrusion, we compounded 75/25, 50/50 and 25/75 wt% PLA/PBAT compounds, and tested a 100% PBAT-based system as reference. All the polymers and the foaming agent were used as received.

### 2.2. Processing of polylactic acid-based foam structures

Foamed sheets were produced with a Labtech 25–30C single-screw extruder (Labtech Engineering Co., Ltd., Thailand) equipped with a flat sheet die for sheet production. The polymer melt after the die reached a tempered roller with a polished surface and was pulled by a pair of pneumatic rollers (Labtech LRC300, Labtech Engineering Co., Ltd., Thailand). The temperature profile was 155/160/175/190/190/190 °C. The width of the die was 300 mm. The flat sheet die has an adjustable gap of 4 mm. Screw rotation speed was 80 rpm. The temperature of the tempered, polished roller was 40 °C. The speed of the roller was 0.4 m/min and the drawing speed was 0.8 m/min. No winding was used. Prior to processing, the semi-crystalline PLAs were dried in a Faithful WGLL-125 BE (Huanghua Faithful Instrument Co., China) hot air oven at 80 °C for 6 h, and the amorphous PLA at 45 °C for 8 h.

### 2.3. Processing of polylactic acid and PBAT-based foam structures

Prior to foaming, the PLA/PBAT blends were compounded with a Labtech Scientific LTE 26–44 modular twin-screw extruder (Labtech Engineering Co., Ltd., Thailand). The extruder had a screw diameter of 26 mm, and the L/D ratio of the screw was 44. The temperature profile was 170/175/175/180/180/180/185/185/190/190/190 °C. The rotation speed of the extruder screws was 50 rpm. A conveyor belt with fans was used to draw and cool the rod-shaped extruded product, which was granulated after solidification. Prior to processing, the semi-crystalline PLAs and PBAT were dried in a Faithful WGLL-125 BE hot air oven at 80 °C for 6 h, and the amorphous PLA at 45 °C for 8 h. Then, the PLA/PBAT blends and the PBAT were foamed according to the foaming process described in section2.2. Prior to foam sheet production, the polymers were re-dried as previously mentioned.

### 2.4. Testing methods

#### 2.4.1. Measurement of density and thickness

The density of the foamed and unfoamed extruded samples was determined from the buoyancy force according to Equation (1) at room temperature (23 ± 2 °C). The measuring medium was distilled water and the analytical balance was an OHAUS Explorer. The measuring range was 110 g and the measuring accuracy was 0.1 mg.

$$\rho = \frac{m_{sa} \cdot \rho_l}{(m_{sa} - m_{sl})} \left[ g / cm^3 \right] \quad (1)$$

where $\rho$ is the density of the sample, $m_{sa}$ is the mass of the sample measured in air, $m_{sl}$ is the mass of the sample measured in distilled water, and $\rho_l$ is the density of distilled water at the measurement temperature. To measure the thickness of the sheet samples, we divided the sheets into 10 equal sections along their width, using a total of 11 measurement points, including the two edges of the sheet. At the defined measuring points, we measured the thickness with a micrometer.

#### 2.4.2. Scanning electron microscopy

Scanning electron microscopy (SEM) images of foamed and unfoamed extruded samples were taken with a JEOL JSM 6380LA microscope (Jeol Ltd., Japan) with an accelerating voltage of 10 kV. The cryogenic fracture surface of the samples was fixed with conductive double-sided carbon adhesive tape. The surface of the sample was sputter coated with gold (JEOL 1200, Jeol Ltd., Japan).

#### 2.4.3. Differential scanning calorimetry

We performed differential scanning calorimetry (DSC) tests with a Q2000 (TA Instruments (USA)) device. The scanned temperature range was 0–200 °C, the heating rate was 5 °C/min, the mass of the samples was 3–6 mg. The measuring atmosphere was $N_2$. We calculated the degree of crystallinity ($\chi_c$[%]) according to Equation (2), where $\Delta H_m$ [J/

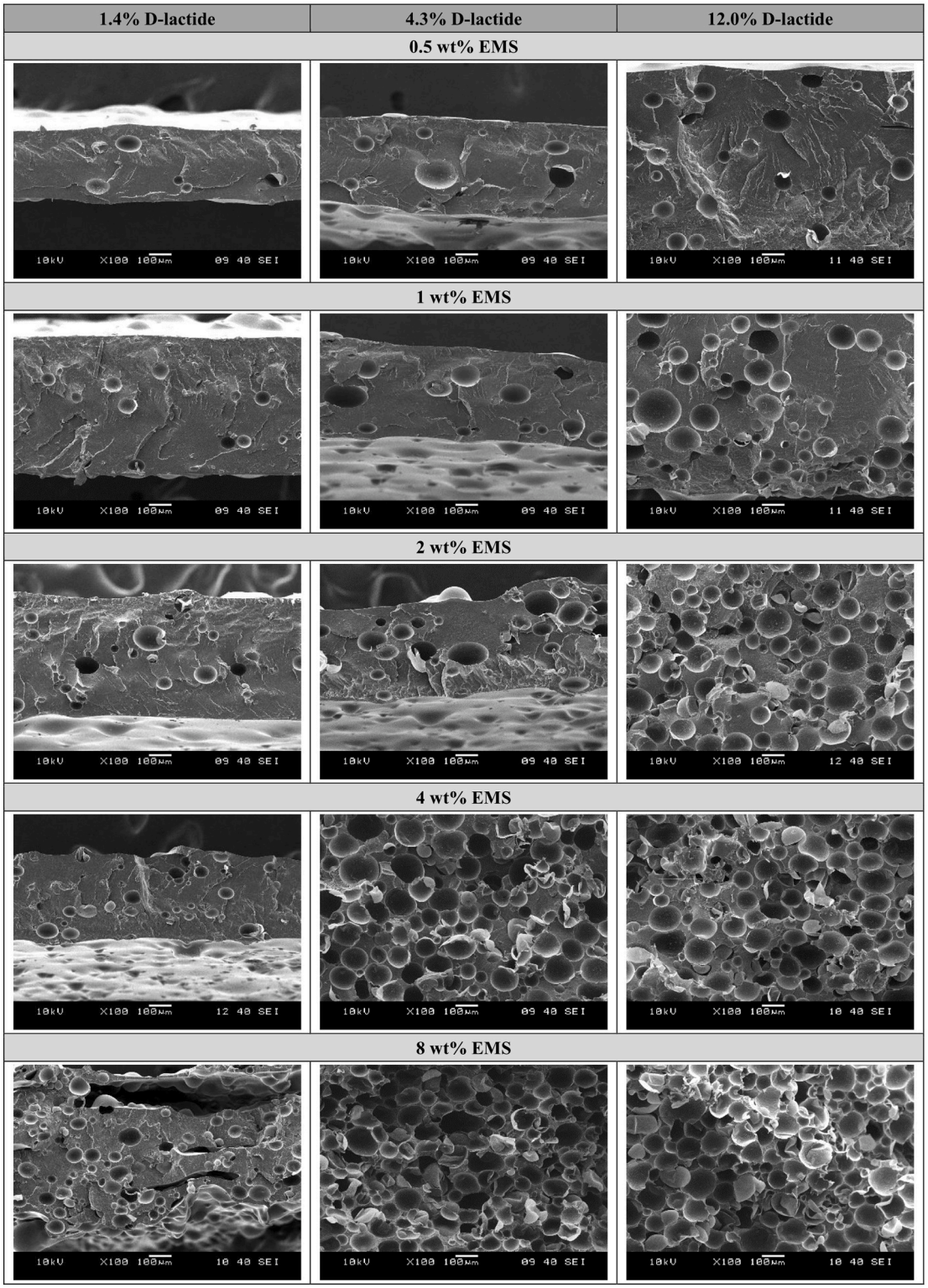


**Fig. 1.** SEM images of the sheet samples (100x magnification).

g] is the melting enthalpy and $PLA_{100\%}$ is the theoretical melting enthalpy of 100% crystalline PLA (93 J/g [23]), and $\alpha$ [−] is the weight fraction of the non-PLA filler. We also calculated the degree of crystallinity created by foam processing ($\chi_{cf}$[%]). We calculated it according to Equation (3), where $\Delta H_{cc}$ [J/g] is the cold crystallization enthalpy of the polymer.

$$\chi_c = \frac{\Delta H_m}{PLA_{100\%}(1-\alpha)} \cdot 100[\%], \tag{2}$$

$$\chi_{cf} = \frac{\Delta H_m - |\Delta H_{cc}|}{PLA_{100\%}(1-\alpha)} \cdot 100[\%], \tag{3}$$

**Table 1**
DSC results of the produced sheet samples (1st heating, heating rate 5 °C/min).

| Sample | $T_g$ | $T_{cc}$ | $\Delta H_{cc}$ | $T_{m1}$ | $T_{m2}$ | $\Delta H_m$ | $X_c$ | $X_{cf}$ |
|---|---|---|---|---|---|---|---|---|
| | °C | °C | J/g | °C | °C | J/g | % | % |
| 1.4%_REF | 60 | 104 | 33.7 | 169 | – | 35.1 | 37.8 | 1.5 |
| 1.4%_8 wt% | 58 | 97 | 31.9 | 168 | – | 35.1 | 38.9 | 3.6 |
| 4.3%_REF | 60 | 114 | 25.7 | 148 | 154 | 25.7 | 27.7 | 0.1 |
| 4.3%_8 wt% | 56 | 105 | 25.5 | 146 | 152 | 27.9 | 30.9 | 2.7 |
| 12.0%_REF | 55 | – | 0.0 | – | – | 0.0 | 0.0 | 0.0 |
| 12.0%_8 wt% | 55 | – | 0.0 | – | – | 0.0 | 0.0 | 0.0 |

#### 2.4.4. Determining the average cell size and cell size distribution

We used scanning electron micrographs to evaluate the foam structures. A minimum of 150 cell diameters were measured for each foam structure with the use of the ImageJ (National Institutes of Health, USA) software. We calculated the mean and standard deviation, and determined the diameter of at least 150 cells using the SEM images and the ImageJ software. Based on these results, frequency and relative frequency were calculated, and relative frequency was plotted as a histogram. Then, a lognormal function was fitted to the relative frequency values.

Determining the damping properties as a function of temperature and frequency.

We performed dynamic mechanical analysis, which showed the damping properties of the foamed and unfoamed samples. During the first DMA test series, the temperature-dependent properties of the samples were investigated. We determined the components of the complex modulus of elasticity, such as the storage modulus (E′), loss modulus (E′′) and loss factor (tanδ) as a function of temperature. We used a DMA Q800 manufactured by TA Instruments (New Castle, DE, USA). The test was performed in dual cantilever mode, with a 35 mm wide support. The width and length of the specimens were 10 mm and 60 mm, respectively, and the thickness of each sample resulted from the expansion of the foamed sheet. The amplitude of periodic bending was 20 μm. When determining the damping properties as a function of temperature, we used a holding time of 5 min at 0 °C. The test was performed between 0 °C and 150 °C with a heating rate of 2 °C/min and a frequency of 1 Hz. Before starting the test, the linear viscoelastic range of the samples was checked by amplitude sweep at 1 Hz and 100 Hz. When determining the damping properties as a function of frequency, we carried out the test at 25 °C. The amplitude of periodic bending was 20 μm. We used a frequency range from 1 Hz to 100 Hz (with 10 measurement points per decade). In the DMA test series to obtain the data for the master curve, we performed frequency sweeps at five isothermals. Bending stress was measured with the clamp type and specimen dimensions in the previous test series. The tests were performed at −5 °C, 5 °C, 15 °C, 25 °C and 35 °C. We used a frequency range from 1 Hz to 100 Hz (with 10 measurement points per decade).

## 3. Results

### 3.1. Analysis of the polylactic acid-based foamed structures

The thickness distribution of the foam sheets along the width of the sheet is an important characteristic, as some mechanical tests require samples with a width of up to 100 mm. Thus, after the production of foam sheets, the expansion of the foam structures was graded by the thickness of the sheets. The thicknesses and SEM images of the foam sheets are shown in Supporting information 1. and Fig. 1. The thickness of the sheets decreases continuously from the edges to the center perpendicular to the direction of production. This characteristic "U" shape is typical of a flat sheet die. The thickness of the sheets in the two outer bands are significantly greater than in the middle section. Based on these results, the samples required for the mechanical tests need to be prepared from the middle part of the foam plates. The thickness of the amorphous Ingeo 4060D samples was the most uniform. Between 20% and 80% of sheet width, the difference in thicknesses is minimal; the variance is between 0.03 and 0.07 mm. This variance shows an increasing trend with increasing EMS content.

Crystalline fraction is an important characteristic of PLA foams. We characterized the morphology of the produced sheet samples using the results from the differential scanning calorimetry. We examined samples with 0 wt% foaming agent and 8 wt% foaming agent. Based on the results (Table 1), not only the reference but the foamed (8 wt%) samples are amorphous, because of fast cooling.

The homogeneity of the manufactured foam structures according to cell morphology was rated by the distribution of the average cell size.

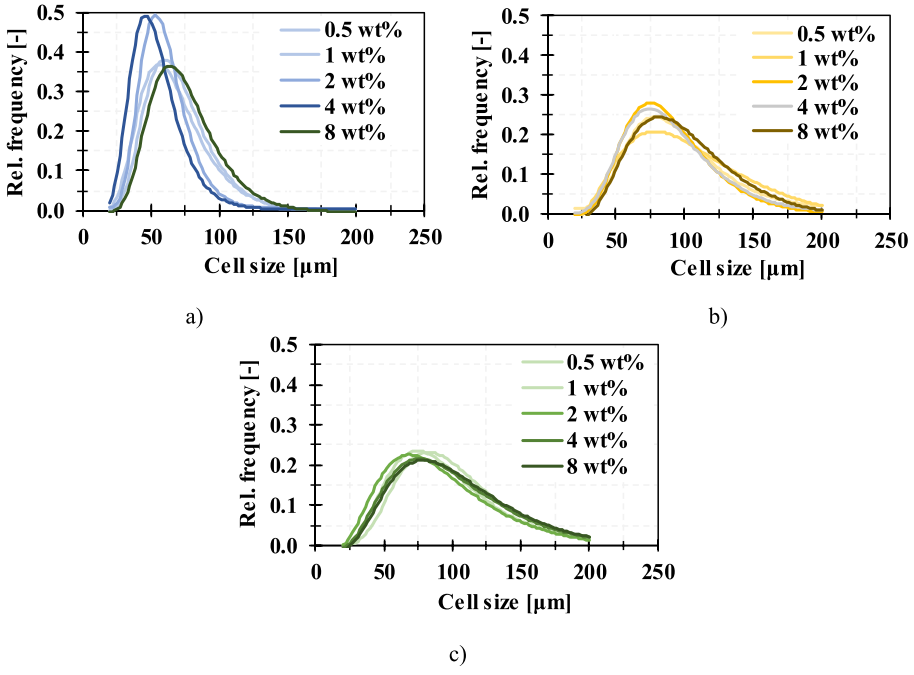


**Fig. 2.** Cell size distribution of foamed sheet PLA samples with a) 1.4%, b) 4.3% and c) 12.0% D-lactide content.

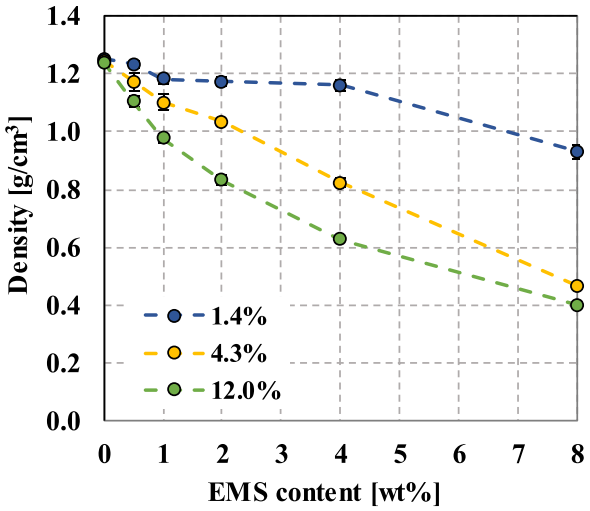


**Fig. 3.** PLA-based foam densities as a function of foaming agent content.

These results are shown in Fig. 2. The cell size distributions are almost identical for all three PLA types with increasing EMS content. Also, the cell size distribution curves of PLAs with medium (4.3%, Fig. 2. b) and high (12.0%, Fig. 2. c) D-lactide content are similar. For these two PLA types, the relative frequency of cell sizes are also nearly the same. In contrast, the cell size distribution curve of PLA foams with small (1.4%, Fig. 2. a) D-lactide content differs significantly. The cell size distribution curves of PLA types with medium and high D-lactide content are flatter, the range of the most frequent cell sizes is wider (60–120 μm) than for the low D-lactide content PLA (40–80 μm). The average cell size was 55.4±1.8 μm for the PLA with low D-lactide content, while it was 84.9± 2.8 μm for the PLA with medium D-lactide content and 87.6 ± 2.9 μm for the high D-lactide content PLA. The micro-sized beads were able to expand to a greater extent in PLAs of higher D-lactide content than in the PLA with low D-lactide content. This phenomenon is related to the viscosity of the polymers. Based on our previous result [3], the shear viscosities of the PLA samples show a slight deviation relative to one another. Complex viscosity decreases with increasing shear rate measured at 190 °C. The complex viscosities of Ingeo 2003D, Ingeo 4032D and Ingeo 4060D were 2344 Pas, 2344 Pas, and 2336 Pas, respectively. EMS can most easily expand in Ingeo 4060D, since it has the lowest viscosity. We also measured the foam density of the samples (Fig. 3). The densities are in good correlation with the SEM images and the cell size distribution results. The lowest density was achieved with Ingeo 4060D with 8 wt% EMS foaming agent (0.401 g/cm$^3$).

**Table 2**
The results of DMA tests with different EMS content.

| Property | Unit | PLA with 12.0% D-lactide content foamed with EMS | | | | | |
|---|---|---|---|---|---|---|---|
| | | 0 wt % | 0.5 wt % | 1 wt % | 2 wt % | 4 wt % | 8 wt % |
| E' (25 °C) | MPa | 2476 | 1491 | 1146 | 1127 | 812 | 384 |
| E' ($T_g$+10 °C) | MPa | 5.7 | 8.9 | 4.7 | 7.6 | 4.6 | 5.5 |
| $T_g$ (from $tan\delta_{MAX}$) | °C | 58.7 | 58.5 | 57.9 | 57.3 | 57.6 | 56.1 |
| $tan\delta_{MAX}$ | – | 2.68 | 2.46 | 1.93 | 1.41 | 1.27 | 0.81 |

### 3.2. Temperature-dependent damping properties of polylactic acid-based foam structures, and the effect of foaming agent content

To investigate the damping properties of the foamed samples as a function of foaming agent content, we chose samples produced with PLA containing 12.0% D-lactide, because of our manufacturing technology experience and also, density reduction was the greatest in this case. We investigated the damping properties of the produced foam structures by dynamic mechanical analysis. The polymers showed maximum damping capacity in the glass transition region. Therefore, the principle of designing a polymer system for damping applications is choosing a polymer whose $T_g$ is close to the operating temperature of the application. For example, polyvinyl acetate (PVA) has a $T_g$ of 30 °C and therefore can be used for vibration damping at normal ambient temperatures. PVA-based anti-vibration coatings are widely used in many industries. Before DMA testing, it is necessary to check whether the response functions of the polymer are linear [17]. The response of a polymer to excitation is a function of three parameters (temperature, frequency and amplitude). If the response of a given material depends on only two parameters, the descriptive equation is linear. Thus, it is necessary to examine the range of linear viscoelasticity (LVE). In the range of LVE, the storage modulus is constant for the amplitude used. Choosing 10% of the limit of the constant amplitude range is thus appropriate [24]. Supporting information 2 presents the results of the examination of the viscoelastic range. Based on the results, the amplitudes tested at 1 Hz are constant over the entire tested range, while the storage modulus drops drastically above 160 μm during amplitude sweeping at 100 Hz. Based on the results, the rounded value for the amplitude is 20 μm.

With the specified amplitude, we carried out a DMA test as a function of temperature, and determined the storage and loss moduli, and tanδ (Fig. 4). The glass transition temperature of the samples was calculated from the loss modulus. We determined the storage modulus of the

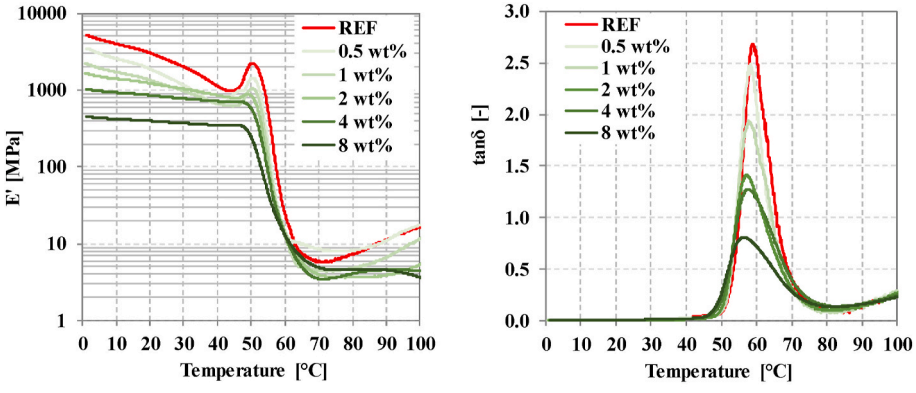


a) b)

**Fig. 4.** PLA with 12.0% D-lactide content foamed with expandable microspheres a) specific storage modulus, b) specific tanδ as a function of temperature (heating rate 2 °C/min).

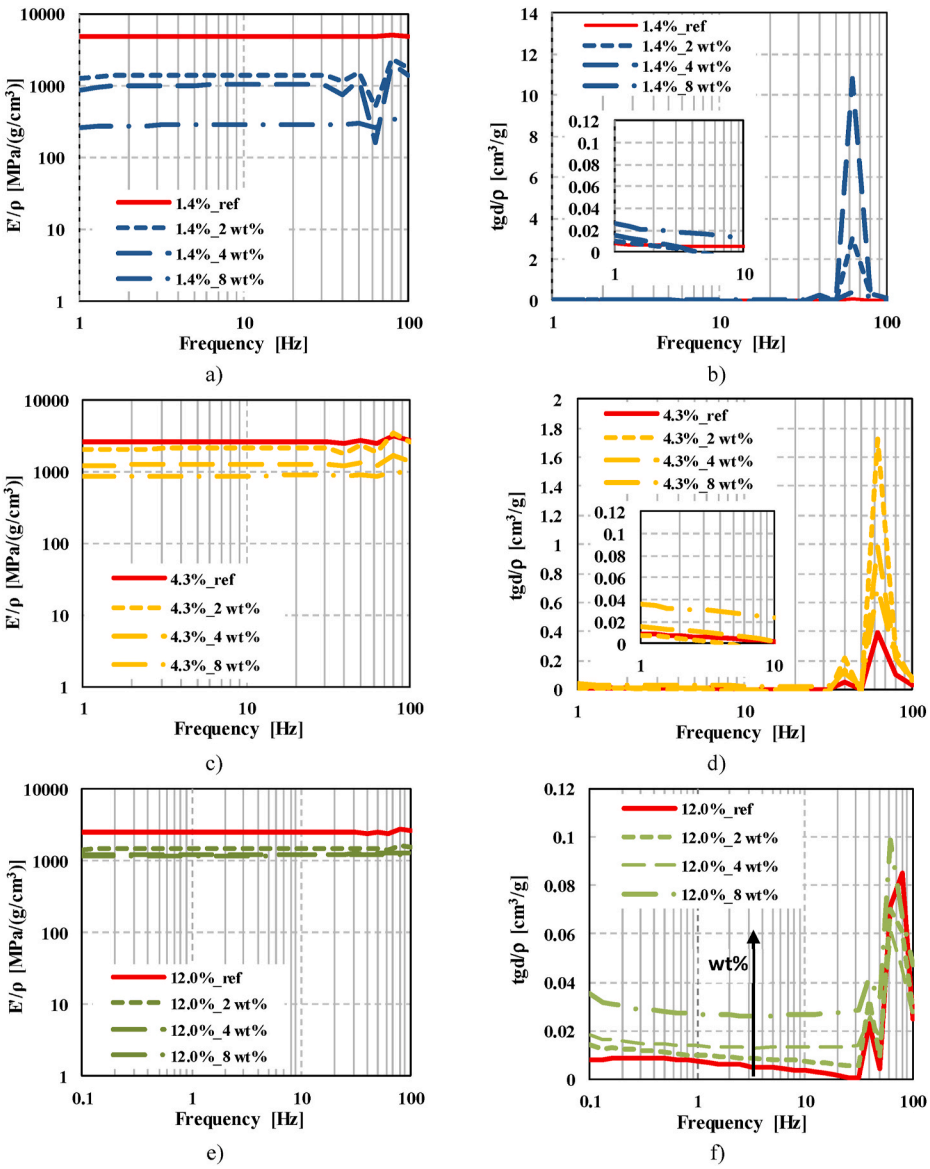


**Fig. 5.** DMA results of the PLA-based samples with a) and b) 1.4% (4032D), c) and d) 4.3% (2003D), e) and f) 12.0% (4060D) D-lactide content: moduli and specific loss factors as a function of the applied frequency (at 25 °C).

samples at room temperature (25 °C) and above the glass transition temperature ($T_g$+10 °C). With the use of these results, the change in mechanical properties due to a temperature increase can be investigated. These results are shown in Table 2.

Under dynamic stress, if the frequency of the applied stress is constant, the polymer behaves as a rigid body under $T_g$. The storage modulus is maximal; the loss factor is minimal (Fig. 4.). As the temperature gradually rises, the smallest segments begin to move first, as the energy required for this is lower. As the temperature increases, both the loss modulus and the loss factor increase. As the temperature continues to rise, more and larger segments are able to move due to the applied frequency and force [4]. Based on Fig. 4 a), the storage modulus decreased above $T_g$. This is because the movement of high molecular weight polymer chains is limited at low temperatures. In the case of the unfoamed sample, the largest decrease in the storage modulus is from 2476 MPa to 5.7 MPa (Table 2). The storage modulus decreases at 25 °C due to the foaming agent. In the case of foamed samples, the decrease in the initial modulus is smaller and it decreases above $T_g$ + 10 °C to the order of magnitude of the storage modulus of the unfoamed sample (5.7 MPa). The glass transition temperature, which is determined from the maximum value of the loss factor, also decreases. The storage modulus increases immediately before the glass transition temperature range. The greatest increase can be observed in the unfoamed reference sample. This increase is reduced with increasing foaming agent content. The reason for this is that an internal stress remains in the sheet products from the flat sheet extrusion process, which can relax during the test as the temperature rises. The damping properties of the manufactured samples were rated by tanδ as a function of temperature. The larger the peak value and width of tanδ, the greater the attenuation. Fig. 4 b) shows the value of tanδ as a function of temperature. These results are consistent with the results of Javadi et al. [1]. The authors explained that the phenomenon was caused by the presence of cavities/cells in the foam structure.

### 3.3. *Frequency-dependent damping properties of polylactic acid foam structures, the effect of D-lactide content*

After determining the temperature-dependent damping properties, we tested the damping properties at room temperature as a function of the excitation frequency (frequency sweep). A typical application

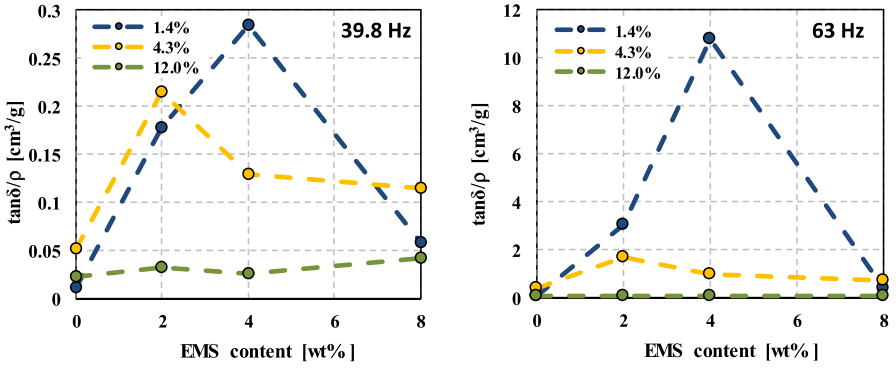


a) b)

**Fig. 6.** Specific loss factors for PLA-based sheets and foams containing 1.4% (4032D), 4.3% (2003D) and 12.0% (4060D) D-lactide, as a function of foaming agent content (EMS) used a) at 39.8 Hz, b) at 63 Hz (at 25 °C).

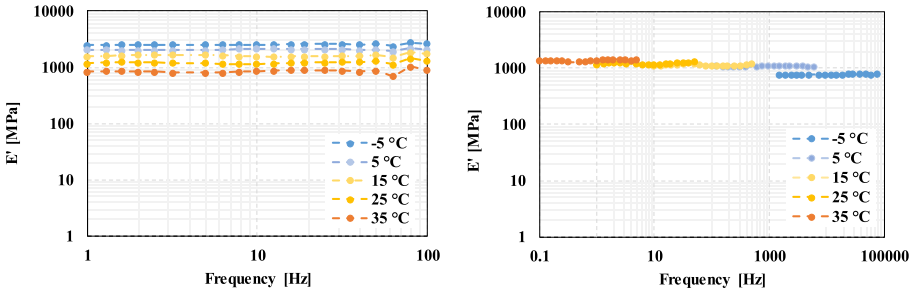


a) b)

**Fig. 7.** a) Storage modulus of a PLA-based foam structure containing 2 wt% EMS at different isothermal temperatures, b) the resulting master curve of the storage modulus (at 25 °C).

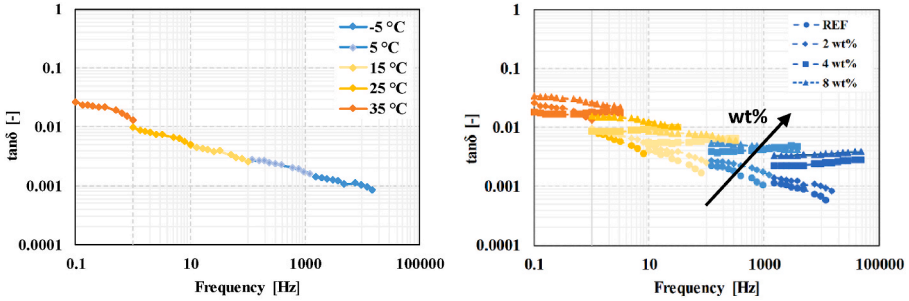


a) b)

**Fig. 8.** a) The resulting master curve of the damping factor of a PLA-based foam structure containing 2 wt% EMS, b) the resulting master curves of the damping factors for different foaming agent contents (at 25 °C).

temperature for polylactic acid is below the glass transition temperature (50–70 °C [12]), therefore, it is recommended to perform DMA at room temperature as a function of frequency. This way, the damping properties of the samples below the glass transition temperature can be rated. Fig. 5 shows the specific storage modulus (E'/ρ) and the specific loss factor (tanδ/ρ) as a function of frequency, in the measuring range of 1 Hz–100 Hz. With increasing EMS content, the specific storage modulus decreases, regardless of D-lactide content. This significant decrease of specific storage modulus is a result of the EVA content of the foaming agent [25]. However, above 30 Hz, at 39.8 Hz and 63 Hz, the loss factor increases, i.e. the damping capacity of the material increases (Fig. 5 b), d), f)). Keller [26] has reported a similar phenomenon in the case of expanded polystyrene. The increase of tanδ can be originated from the loss modulus (E''). Loss modulus is the viscous response of the material, proportional to the irrecoverable or dissipated energy [27]."

The loss factor decreases as the D-lactide content of the PLA increases (Fig. 6). However, in the case of the sample with a highest D-lactide content, it can be clearly seen that in the range below 30 Hz, the value of tanδ/ρ shows an increasing tendency with increasing amounts of EMS.

In the next step, we extended the frequency-dependent damping properties at room temperature using the TTS method—we performed frequency sweep tests on a series of isothermals. For this experiment, we chose the foams with the best density reduction—the foams produced from PLA with 12.0% D-lactide content. Fig. 6 shows the resulting

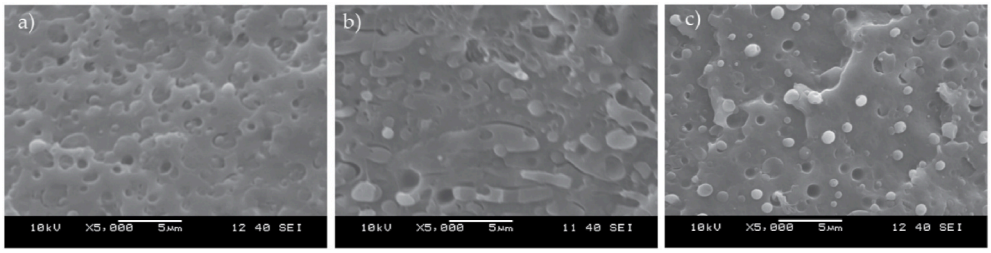


**Fig. 9.** SEM images of PBAT/PLA blends a) 75/25 wt%, b) 50/50 wt%, c) 25/75 wt% with 8 wt% EMS foaming agent.

storage modulus as a function of the frequency between 1 Hz and 100 Hz at different temperatures. We applied the TTS method to these measurement results. We chose the reference temperature to be 25 °C, and obtained the master curve according to Fig. 7 b). The applied shifting was manual. With the use of the same offset values for the loss factor, we obtained the master curve according to Fig. 8 a). Fig. 8 b) shows the resulting master curves of the foam structures produced with 0, 2, 4 and 8 wt% EMS. The results indicate that with an increase of EMS content in the extended frequency range, the damping factor of the foam structures increases in the range of 0.1 Hz–20 000 Hz. In vehicles, lightweight polyurethane foams are used for noise control. PU foams has tanδ maxima around $10^7$ Hz, 0.35.

### *3.4. Possibilities to increase the damping capability of biopolymer foam structures*

In some cases, the requirement for vibration damping cannot be met with commercially available homopolymers alone. It is difficult to produce a suitable homopolymer with a suitable $T_g$ and adequate mechanical properties. Moreover, a homopolymer usually has a narrow range of glass transition temperature. It is typically necessary to modify the polymer system for vibration damping applications—the glass transition region and the viscoelastic properties of the polymers has to be adjusted properly. From this point of view, the blending of polymers may be advantageous [4]. Based on the literature, PLA-based blends with synthetic/non-degradable thermoplastics are often researched, such as PLA/rubber, PLA/PU blends, and PLA/PE blends. Although these synthetic/non-degradable thermoplastics are non-degradable, they can still be beneficial for the environment and energy vise as they increase the toughness of PLA [28]. Mi et al. [29] examined PLA/TPU blends, and it's foamability. In their work, they added 25-50-70 wt% TPU to PLA, which formed an immiscible blend. As a result of DMA measurements, two well-distinguishable tanδ peaks were characterized. The tanδ peak of TPU is in the negative temperature range and decreased with increasing PLA content. The other tanδ peak belongs to the PLA decreased with increasing TPU content. The viscosity of the blends increased with increasing TPU content. As a result of microcellular injection molding, it was found that the foam samples containing 25 and 75 wt% TPU had a similar cell structure as the reference PLA and TPU foams. While samples containing 50% TPU have smaller cell sizes and porosity, it is believed that the island phase of PLA in the TPU matrix prevented cell growth. The foams thus produced have a porosity of 49–79%. In their work, Zhou et al. [30] set a goal to improve the toughness, rheological properties, and foamability of PLA by creating PLA/LDPE blends. The addition of LDPE to PLA greatly increased the viscosity of PLA, which led to a decrease in the cell size and expansion of the foam structures during supercritical foaming at a production temperature of 105 °C. In the work of Zhao et al. [31], HDPE was added to PLA, where HDPE content in PLA also caused an increase in viscosity due to the higher viscosity of HDPE. The presence of 5 wt% and 10 wt% HDPE during foaming (at 110 °C) in the PLA-based system led to a complex cellular structure due to the altered cell nucleation mechanism caused by the dispersed HDPE phase. We chose PLA with a D-lactide content of 4.3% because it proved to be suitable for both damping and foaming. We wanted to find the energy absorption properties of foams produced from blends of this PLA and other biopolymers, which have a lower $T_g$. We chose PBAT, which is considered as a promising biopolymer, flexible and tough biopolymer that improves processability and foamability [28,32–34]. We examined how the presence of PBAT changes the energy absorption properties of the polymer foam. The chosen PBAT dosages were 25, 50 and 75 wt% and we also tested the 100% PBAT system as reference. The resulting blends are immiscible, as can be seen on the cryogenic fracture surfaces in SEM images (Fig. 9). Average PBAT droplet sizes below 1 μm (0.892 ± 0.246 μm) were achieved with the 75% PLA/25% PBAT blend (Fig. 9 a). However, phase inversion was detected in the case of the 75% PBAT/25% PLA blend, where the average PLA droplet size was also below 1 μm (0.741 ± 0.174 μm) (Fig. 9 c). These results correlate with previous results of Kumar et al. [35], Nofar et al. [36] and Ding et al. [37]. In the case of the 50% PLA/50% PBAT blend, a co-continuous phase was formed [33], which can be explained by the rheological properties of the materials. The melt flow rate of PLA and PBAT was 2.0 g/10 min [38] and 3.3 g/10 min (190 °C, 2.16 kg) [39], respectively.

We investigated the damping properties of the unfoamed samples by

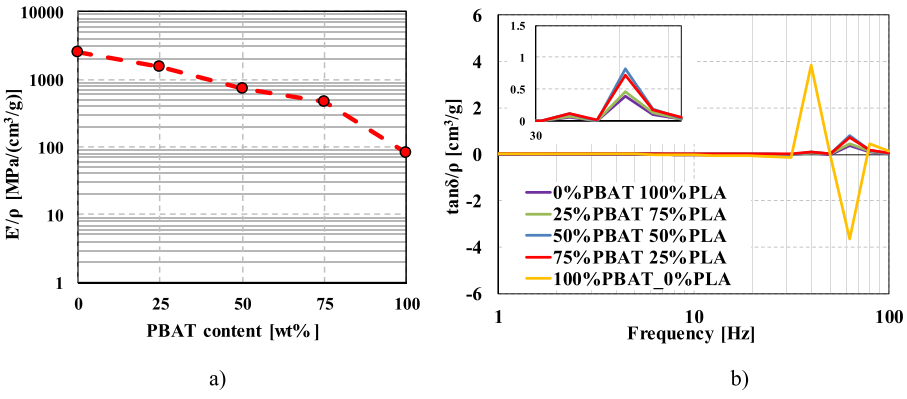


**Fig. 10.** PLA and PLA-based blends and PBAT a) specific storage modulus of at 1 Hz as a function of PBAT content b) loss factor as a function of frequency (at 25 °C).

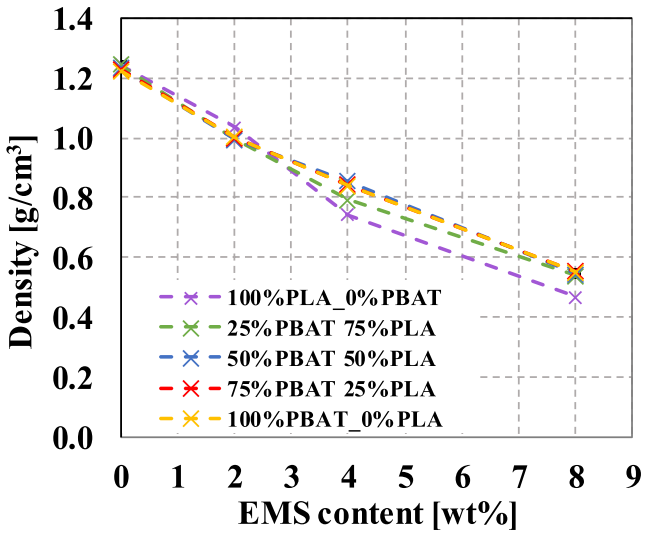


**Fig. 11.** Density of PLA-based blends and PBAT as a function of EMS foaming agent content.

DMA. Fig. 10 a) shows the specific storage modulus of the manufactured foam sheets, and Fig. 10 presents the specific loss factor as a function of PBAT content. The storage modulus shows a decreasing tendency in the unfoamed reference samples, and these results indicate the presence of PBAT in the PLA system. This decreasing tendency is because at room temperature PLA is in its glassy state, and PBAT is in its rubbery state; therefore, its segment mobility is increased. Fig. 10 b) shows the tanδ results as a function of the applied frequency. The 100% PBAT sample shows outstanding damping capacity with a loss factor of 4.77, compared to the 100% PLA sample (tanδ = 0.48). This is due to its high damping ability, related to the ease of movement of side chains, side groups, and chain segments [4]. Among the blends, 50% PLA with 50% PBAT has the highest loss factor (tanδ = 1.01). This most probably originates from the co-continuous phase morphology (see Fig. 9) .

We produced foamed sheets from the blends with 2, 4, and 8 wt% Tracel G 6800 MS foaming agent, and achieved a density of 0.467 ± 0.005 g/cm$^3$ with the use of 8 wt% foaming agent (Fig. 11). With increasing PBAT content, density increased to 0.55 g/cm$^3$ at 8 wt% foaming agent content. The complex viscosity of the neat PLA is lower than the viscosity of neat PBAT at a lower shear rate. However, at higher shear rate, the viscosity of PBAT is lower than PLA, because PBAT has a shear-thinning characteristic [40]. The viscosity of the PLA/PBAT blends changes. In the case of PLA/PBAT (75/25%) at lower frequency range, the complex viscosity of the PLA is increased by PBAT content [41]. When 5-10-15-20-30 wt% PBAT was added to PLA, it was found that at lower shear rates, the viscosity of the PLA/PBAT blends increases with the naming of the PBAT content to the reference PLA [40]. During foaming, the shear rate of cell expansion is in the order of 5 s$^{-1}$ [42]. Thus, our foam density results are presumably related to the lower viscosity of PLA and proved to be more favorable than the higher viscosity of the PLA/PBAT blends.

We also investigated the damping properties of the foamed samples by DMA (Fig. 12). The maxima of tanδ changed when foaming agent was added to the PLA. With 8 wt% foaming agent, the specific loss factor increased to 6.08. In foamed PBAT systems, 8 wt% foaming agent also increased the specific loss factor to 8.55. For blended systems, foaming did not prove to be a successful method of increasing damping properties in the measured frequency range.

## 4. Conclusions

We investigated the damping properties of homogeneous cellular biopolymer-based foam structures with the use of thermally expandable microspheres. We measured the density of the resulting foam structures, expansion characteristics (sheet thickness) and cell size distribution, and took into account the effect of the D-lactide content of the polylactic acid. We determined the required parameters of the DMA test and successfully extended the frequency-dependent properties of the materials. We found that the damping properties of a homogeneous, closed-cell foam structure produced with thermally expandable microspheres increase in the range of 0.1–20 000 Hz as a function of foaming agent content. We also produced foamed sheets from the PLA/PBAT blends. The results indicate that the presence of PBAT in the PLA system has a plasticizing effect. The storage modulus of unfoamed reference samples shows a decreasing tendency as a function of frequency. In the case of foamed blends, tanδ was reduced in general. For systems containing 75 and 100 wt% PBAT, tanδ increased again, therefore the use of a PBAT/PLA blend is only

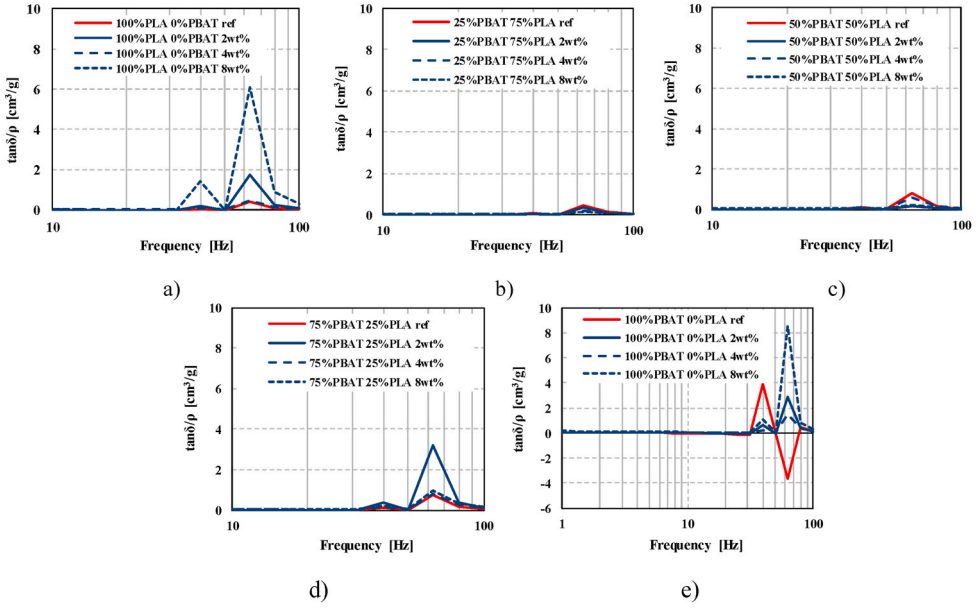


**Fig. 12.** Specific storage modulus and specific loss factor as a function of frequency in the case of a) 100% PLA-based foams, b) 75% PLA/25% PBAT-based foams, c) 50% PLA/50% PBAT-based foams, d) 25% PLA/75% PBAT-based foams, e) 100% PBAT-based EMS foams (at 25 °C).

advantageous above 75 wt% PBAT to improve the damping ability of the foamed samples.

## Funding

This paper was "Supported by the ÚNKP-20-3 New National Excellence Program of the Ministry for Innovation and Technology from the source of the National Research, Development and Innovation Fund" and "János Bolyai Research Scholarship of the Hungarian Academy of Sciences". This research was also supported by the National Research, Development and Innovation Office (NVKP_16-1-2016-0012). This research was supported by the National Research, Development and Innovation Office NKFIH, K 132462. The research reported in this paper and carried out at BME has been supported by the NRDI Fund (TKP2020 IES, Grant No. BME-IE-NAT) based on the charter of bolster issued by the NRDI Office under the auspices of the Ministry for Innovation and Technology.

## Credits

Conceptualization, Ákos Kmetty; methodology, Ákos Kmetty and Katalin Litauszki; formal analysis, Ákos Kmetty and Katalin Litauszki; investigation; writing—original draft preparation, Ákos Kmetty and Katalin Litauszki; writing—review and editing, Ákos Kmetty and Katalin Litauszki.

## Declaration of competing interest

The authors declare that they have no known competing financial interests or personal relationships that could have appeared to influence the work reported in this paper.

## Acknowledgements

We would like to thank Tramaco GmbH (Germany) and to INTERDIST Kft. for the Tracel G 6800 MS foaming agent.

## Appendix A. Supplementary data

Supplementary data to this article can be found online at https://doi.org/10.1016/j.polymertesting.2021.107347.

## Data availability

The raw/processed data required to reproduce these findings cannot be shared at this time as the data also forms part of an ongoing study.

## References

[1] A. Javadi, J.A. Kramschuster, S. Pilla, J. Lee, S. Gong, L.-S. Turng, Processing and characterization of microcellular PHBV/PBAT blends, Polym. Eng. Sci. 50 (2010) 1440–1448.
[2] V.A. Szabó, G. Dogossy, Investigation of flame retardant rPET foam, Period. Polytech. - Mech. Eng. 64 (2020) 81.
[3] Á. Kmetty, K. Litauszki, Development of poly(lactide acid) foams with thermally expandable microspheres, Polymers 12 (2020) 463.
[4] B.C. Chakraborty, D. Ratna, Polymers for Vibration Damping Applications, Elsevier, Amsterdam, Netherlands, 2020.
[5] Á. Kmetty, M. Tomin, T. Bárány, T. Czigány, Static and dynamic mechanical characterization of cross-linked polyethylene foams: the effect of density, Express Polym. Lett. 14 (2020) 503.
[6] A.J. Brammer, D.R. Peterson, Vibration, mechanical shock, and impact, in: M. Kutz (Ed.), Standard Handbook of Biomedical Engineering & Design, McGRAW-HILL, New York, NY, USA, 2003.
[7] F. Briatico-Vangosa, M. Benanti, L. Andena, C. Marano, R. Frassine, M. Rink, C. Visentin, P. Bonfiglio, F. Pompoli, N. Prodi, Dynamic Mechanical Response of Foams for Noise Control, Regional Conference Graz 2015 – Polymer Processing Society, AIP Conference Proceedings, 2016. Graz, Austria.
[8] J. Park, S. Choi, H.M. Jung, Measurement and analysis of vibration levels for truck transport environment in Korea, Appl. Sci. 10 (2020) 1–19.
[9] M.P. Kevin, DMA Applications to Real Problems: Guidelines, Dynamic Mechanical Analysis: A Practical Introduction, CRC Press, Boca Raton, 1999.
[10] Y. Fu, I.I. Kabir, G.H. Yeoh, Z. Peng, A review on polymer-based materials for underwater sound absorption, Polym. Test. (2021) 96.
[11] N. Gupta, S.E. Zeltmann, D.D. Luong, M. Doddamani, Foam testing, in: Chun-Hway Hsueh (Ed.), Handbook of Mechanics of Materials, Springer, Singapore, 2019.
[12] R. Auras, L.-T. Lim, S.E.M. Selke, H. Tsuji, Poly(Lactic Acid) Synthesis, Structures, Properties, Processing and Applications, Wiley, New Jersey, 2011.
[13] C. Xu, X. Luo, X. Lin, X. Zhuo, L. Liang, Preparation and characterization of polylactide/thermoplastic konjac glucomannan blends, Polymer 50 (2009) 3698–3705.
[14] M. Joo, R. Auras, E. Almenar, Preparation and characterization of blends made of poly(l-lactic acid) and β-cyclodextrin: improvement of the blend properties by using a masterbatch, Carbohydr. Polym. 86 (2011) 1022–1030.
[15] A. Kramschuster, S. Pilla, S. Gong, A. Chandra, L.-S. Turng, Injection molded solid and microcellular polylactide compounded with recycled paper shopping bag fiber, Int. Polym. Process. 22 (2007) 436.
[16] S. Pilla, A. Kramschuster, J. Lee, G.K. Auer, S. Gong, L.-S. Turng, Microcellular and solid polylactide–flax fiber composites, Compos. Interfac. 16 (2012) 869–890.
[17] C. Kwang Soo, Viscoelasticity of Polymers: Theory and Numerical Algorithms, Springer, Dordrecht, 2016.
[18] T. Standau, C. Zhao, S. Murillo Castellón, C. Bonten, V. Altstädt, Chemical modification and foam processing of polylactide (PLA), Polymers 11 (2019) 306.
[19] L.L.C. NatureWorks, Technical Data Sheet Ingeo Biopolymer 2003D, 4032D and 4060D, NatureWorks LLC, Minnetonka Blvd., Minnetonka, MN 55345, 2019, 15305.
[20] K. Bocz, B. Szolnoki, A. Farkas, E. Verret, D. Vadas, K. Decsov, G. Marosi, Optimal distribution of phosphorus compounds in multi-layered natural fabric reinforced biocomposites, Express Polym. Lett. 14 (2020) 606.
[21] K. Litauszki, Á. Kmetty, Extrusion foaming of poly(lactic acid) with thermally expandable microsphers, in: SPE Foams 2019 Conference, SPE, Valladolid, Spain, 2019, pp. 1–5.
[22] BASF, Techical datasheet, Ecoflex F Blend C1200, BASF, Ludwigshafen, Deutschland, 2013.
[23] S. Hajba, T. Tábi, Cross effect of natural rubber and annealing on the properties of poly(lactic acid), Period. Polytech. - Mech. Eng. 63 (2019) 270–277.
[24] I. Agirre-Olabide, J. Berasategui, J.M. Elejabarrieta, M.M. Bou-Ali, Characterization of the linear viscoelastic region of magnetorheological elastomers, J. Intell. Mater. Syst. Struct. 25 (2014) 2074–2081.
[25] R.K. Singla, M.T. Zafar, S.N. Maiti, A.K. Ghosh, Physical blends of PLA with high vinyl acetate containing EVA and their rheological, thermo-mechanical and morphological responses, Polym. Test. 63 (2017) 398–406.
[26] J.-H. Keller, V. Altstädt, Influence of Mid-stress on the Dynamic Fatigue of a Light Weight EPS Bead Foam, e-Polymers, 2019, p. 19.
[27] V. Placet, E. Foltête, Is dynamic mechanical analysis (DMA) a non-resonance technique? Eur. Phys.J.Conf 6 (2010) 1–8.
[28] M. Nofar, D. Sacligil, P.J. Carreau, M.R. Kamal, M.-C. Heuzey, Poly (lactic acid) blends: processing, properties and applications, Int. J. Biol. Macromol. 125 (2019) 307–360.
[29] H.Y. Mi, M.R. Salick, X. Jing, B.R. Jacques, W.C. Crone, X.F. Peng, L.S. Turng, Characterization of thermoplastic polyurethane/polylactic acid (TPU/PLA) tissue engineering scaffolds fabricated by microcellular injection molding, Mater Sci Eng C Mater Biol Appl 33 (2013) 4767–4776.
[30] H. Zhou, M. Zhao, Z. Qu, J. Mi, X. Wang, Y. Deng, Thermal and rheological properties of poly(lactic acid)/low-density polyethylene blends and their supercritical CO2 foaming behavior, J. Polym. Environ. 26 (2018) 3564–3573.
[31] M. Zhao, X. Ding, J. Mi, H. Zhou, X. Wang, Role of high-density polyethylene in the crystallization behaviors, rheological property, and supercritical CO2 foaming of poly (lactic acid), Polym. Degrad. Stabil. 146 (2017) 277–286.
[32] N. Mohammadreza, S. Dilara, C.J. Pierre, K.R. Musa, H. Marie-Claude, Poly (lactic acid) blends: processing, properties and applications, Int. J. Biol. Macromol. 125 (2019) 307–360.
[33] K. Li, J. Peng, L.-S. Turng, H.-X. Huang, Dynamic rheological behavior and morphology of polylactide/poly(butylenes adipate-co-terephthalate) blends with various composition ratios, Adv. Polym. Technol. 30 (2011) 150–157.
[34] L. Aliotta, I. Canesi, A. Lazzeri, Study on the preferential distribution of acetyl tributyl citrate in poly(lactic) acid-poly(butylene adipate-co-terephthalate) blends, Polym. Test. 98 (2021).
[35] M. Kumar, S. Mohanty, S.K. Nayak, M. Rahail Parvaiz, Effect of glycidyl methacrylate (GMA) on the thermal, mechanical and morphological property of biodegradable PLA/PBAT blend and its nanocomposites, Bioresour. Technol. 101 (2010) 8406–8415.
[36] M. Nofar, A. Tabatabaei, H. Sojoudiasli, C.B. Park, P.J. Carreau, M.C. Heuzey, M. R. Kamal, Mechanical and bead foaming behavior of PLA-PBAT and PLA-PBSA blends with different morphologies, Eur. Polym. J. 90 (2017) 231–244.
[37] Y. Ding, B. Lu, P. Wang, G. Wang, J. Ji, PLA-PBAT-PLA tri-block copolymers: effective compatibilizers for promotion of the mechanical and rheological properties of PLA/PBAT blends, Polym. Degrad. Stabil. 147 (2018) 41–48.
[38] Á. Kmetty, K. Litauszki, D. Réti, Characterization of different chemical blowing agents and their applicability to produce poly(lactic acid) foams by extrusion, Appl. Sci. 8 (2018) 1960.
[39] L.B. Tavares, N.M. Ito, M.C. Salvadori, D.J. dos Santos, D.S. Rosa, PBAT/kraft lignin blend in flexible laminated food packaging: peeling resistance and thermal degradability, Polym. Test. 67 (2018) 169–176.

[40] S.-Y. Gu, K.Z. Jie Ren, H. Zhan, Melt rheology of polylactide/poly(butylene adipate-co-terephthalate) blends, Carbohydr. Polym. 74 (2008) 79–85.

[41] M. Nofar, A. Maani, H. Sojoudi, M.C. Heuzey, P.J. Carreau, Interfacial and rheological properties of PLA/PBAT and PLA/PBSA blends and their morphological stability under shear flow, J. Rheol. 59 (2015) 317–333.

[42] S.-T. Lee, Foam Extrusion: Principles and Practice, CRC Press, Boca Raton, 2014.